(1)

N E L Report No 465

NATIONAL ENGINEERING LABORATORY

Linear Fracture Mechanics - What It Is, What It Does

L. P. POOK

MINISTRY OF TECHNOLOGY AUGUST 1970

MINISTRY OF TECHNOLOGY

NATIONAL ENGINEERING LABORATORY

LINEAR FRACTURE MECHANICS - WHAT IT IS, WHAT IT DOES

by

L. P. Pook, B.Sc., Ph.D.

(Materials Group: Strength of Components and Fatigue Division)

SUMMARY

This report is intended to assist non-specialists in understanding the numerous specialist papers on linear elastic fracture mechanics. The main concepts are described, and the various terms and conventions used are explained. Advanced mathematical techniques are used in fracture mechanics; some of these are described briefly, but results rather than methods are emphasized.

Fracture mechanics developed from the study of brittle fractures which had taken place below general yield; it is found that such failures always originate at some type of crack or flaw. Previously, the problem of brittle fracture has been tackled by empirical methods based on service experience but the problem can only be properly understood using fracture mechanics, which is the applied mechanics of crack growth starting from a flaw. Stress analysis of cracked parts leads to the concept of stress intensity factor, which describes the elastic crack tip stress field. A critical value of this factor at which crack growth starts is a useful measure of the fracture toughness, or resistance to brittle fracture of a high strength material, which can be used for material development, quality control, design and failure analysis. The stress intensity factor can also be applied to other types of crack growth such as stress corrosion and fatigue crack growth.

CONTENTS

NOTATION

a	Half length of internal crack or notch, length of surface crack or notch
a_1, a_2, a_3, a_4	Coefficients of stress field expansion
B	Specimen thickness
B_N	Net section thickness
b	Semi-minor axis of ellipse
C	Material constant
c	Semi-major axis of ellipse
E	Young's modulus
G	Shear modulus $E/(2 + 2\nu)$
G_c	Effective surface energy (both crack surfaces)
G_I, G_{II}, G_{III}	Strain energy release rate for different modes
G_{Ic}	Value of G_c for plane strain conditions
K	Rate of increase of K_I with respect to time
K_B	Stress intensity factor for plate bending
K_c	Critical value of K_I
K_E	Value of K_I due to external loads
K_I, K_{II}, K_{III}	Stress intensity factor for different modes
K_{Ia}	K_I for anisotropic materials
K_{Ic}	K_c for plane strain conditions
K_{ISCC}	Critical value of K_I for stress corrosion cracking
K_{max}	Maximum value of K_I during fatigue cycle
K_{mean}	Mean value of K_I during fatigue cycle
K_{min}	Minimum value of K_I during fatigue cycle
K_Q	Provisional value of K_{Ic}
K_R	Value of K_I due to the relief of internal stresses on the introduction of a crack
K_S	Stress intensity factor for plate shear
K_T	Stress concentration factor (σ_{max}/σ)

K_{IIc}	Critical value of K_{II}
ΔK	$K_{max} - K_{min}$
M	Bending moment
m	An exponent
N	Number of cycles
P	Load
P_M, P_Q, P_S	Loads defined in Appendix III and Fig. 13
R	Resistance to crack growth
R	Stress ratio $\sigma_{min}/\sigma_{max}$
r, θ	Polar coordinates (Fig. 1)
r_p	Plastic zone radius
S	Maximum stress rate (rate of increase of stress)
t	Time from zero load
u, v, w	Displacements in x, y, z direction
V	Crack velocity
W	Specimen width
x, y, z	Rectangular coordinates
Y	Stress intensity factor coefficient
α	Correction factor for the geometry of the flaw and structure
γ	Surface energy
δ_c	Critical value of crack opening displacement
λ	Compliance (reciprocal of stiffness)
μ_1, μ_2	Dimensionless elastic constants
ν	Poisson's ratio
ρ	Notch root radius
σ	Gross stress, stress remote from crack or notch
$\sigma_x, \sigma_y, \sigma_z$ σ_r, σ_θ	Stress components in the x, y, z or r, θ directions

σ_{max}	Maximum stress at a notch
σ_{max}	Maximum stress during fatigue cycle
σ_{mean}	Mean stress during fatigue cycle
σ_{min}	Minimum stress during fatigue cycle
σ_Y	Yield stress (taken as the 0.2 per cent proof stress)
$\tau_{xy}, \tau_{xz}, \tau_{yz}$ $\tau_{r\theta}$	Shear stress components.

1. INTRODUCTION

Fracture mechanics has developed from the study of brittle fracture; that is the catastrophic failure of a structure made from a normally ductile material at a load below that necessary to cause general yielding, and without noticeable plastic deformation. Experience shows that brittle fractures always originate at cracks or flaws of various types, for example, fatigue cracks which develop during service, or welding cracks which may be introduced during fabrication. Previously, the problem of brittle fracture was tackled by empirical methods based on service experience but the problem can only be properly understood using fracture mechanics, which is the applied mechanics of crack growth starting from a flaw. Linear elastic fracture mechanics makes use of the elastic stress analysis of a cracked part to define the conditions under which the existing crack, or crack-like flaw, will extend. The basic assumptions are the same as those in strength of materials theory: the material is a homogeneous isotropic continuum (that is microscopic irregularities in structure are neglected); stress is proportional to strain; strains are small; and distortions are neglected. The material is also assumed to be free from self-equilibrating internal stresses. Various modifications can be made to the basic theory to allow for the actual behaviour of real materials.

This report is intended to assist non-specialists in the understanding of the numerous specialist papers on various aspects of linear elastic fracture mechanics which are being published. The symbols used are generally those which are commonly accepted, but some variations will be found in the literature. Table 1 shows customary and SI units used in fracture mechanics. In this report K_c is taken to have a general meaning as any critical value of K_I irrespective of the state of stress, but where K_c is used as a critical value under plane stress conditions, the term 'plane stress K_c' is used. The references cited in each section have been chosen to give an overall view of the subject matter covered; most of the topics are discussed in detail in Reference 1.

2. MODES OF CRACK GROWTH

There are three basic modes of crack surface displacement[2] which can cause crack growth and these are shown in Fig. 1.

(I) The opening mode. The crack surfaces move directly apart; analogous to an edge dislocation.

(II) The edge sliding mode. The crack surfaces move normal to the crack front and remain in the crack plane, also analogous to an edge dislocation.

(III) The shear mode. The crack surfaces move parallel to the crack front and remain in the crack plane; analogous to a screw dislocation[3].

The superimposition of these three modes is sufficient to describe the most general case of crack surface displacement. It is conventional to add roman numerals I, II, III as subscripts to various symbols to indicate the mode. In isotropic materials brittle fracture usually occurs in mode I. Consequently, attention is largely confined to this mode; in this report mode I is implied unless otherwise stated.

In fracture mechanics only the macroscopic mode of crack growth is considered although, on a microscopic scale, fracture is usually a very irregular process. Crack growth which forms shear lips (Fig. 2), often referred to as 'shear fracture', is a combination of modes I and III, but is usually treated in calculations as if it were mode I.

For strictly two-dimensional cases and in shell problems, only modes I and II can exist. However, 'two-dimensional' is often taken to include examples of plates of finite (constant) thickness. Mode II displacements can only exist at internal or mathematically deep external cracks.

3. STRESS INTENSITY FACTOR

Crack surfaces are stress-free boundaries adjacent to the crack tip, and therefore dominate the distribution of stresses in that area[2]. Remote boundaries and loading forces affect only the intensity of the stress field at the crack tip. These fields can be divided into three types corresponding to the three basic modes of crack surface displacement, and are conveniently characterized by the stress intensity factor K (with subscripts I, II, III to denote the mode). K has the dimensions (stress) × (length)$^{\frac{1}{2}}$ and is a function of the specimen dimensions and loading conditions: in general it is proportional to (gross stress) × (crack length)$^{\frac{1}{2}}$. Conventionally K is expressed either in hbar(cm)$^{\frac{1}{2}}$, MN/m$^{\frac{3}{2}}$ or lb/in$^{\frac{3}{2}}$ (sometimes written k.s.i.(in)$^{\frac{1}{2}}$). Expressions for K_I for several configurations[2,4,5] are shown in Fig. 3. When K is known, stresses and displacements near the crack tip can be calculated using standard equations (see Appendix I), the stresses are always inversely proportional to the square root of the distance from the crack tip and become infinite at the crack tip. Provided that only one mode is present the stress intensity factors due to different loadings can be superimposed by algebraic addition; if more than one mode is present the individual stress components and displacements can be similarly superimposed.

Small-scale non-linear effects, such as those due to yielding, microstructural irregularities, internal stresses and local irregularities in the crack surface, do not affect the general character of the stress field and can be regarded as being within the crack tip stress field. They can therefore be neglected in a reasonable approximation[2]. The actual fracture process can similarly be regarded as taking place within the stress field at the crack tip; the concept of stress intensity factor therefore provides a convenient mathematical framework for the study of fracture processes. The effects of residual stresses are discussed in Appendix II.

The representation of a crack tip stress field by a stress intensity factor is a basic concept in fracture mechanics. The term should not be confused with 'stress concentration factor' or 'stress intensification factor', which are terms used to describe the ratio between actual and nominal stress at a discontinuity.

It is found that under increasing load a crack will start to grow (provided that general yielding does not intervene) when K_I reaches a critical value (K_c), and will continue to grow as long as the loading conditions are such that $K_I > K_c$. Under certain conditions K_c can be regarded as a material property and is a convenient measure[6] of the fracture toughness, or resistance to brittle fracture, of a material.

For a crack to grow under static loading, two conditions are necessary and sufficient[7]. There must be sufficient stress available to operate a suitable mechanism of fracture, and the strain energy released by an increment of crack growth must equal or exceed the energy required to form the new crack surfaces. That is,

$$G_I \geqslant G_c$$

G_I = strain energy release rate (1)

G_c = effective surface energy (both surfaces).

In metals the true surface energy is small compared with the additional energy absorbed by the plastic deformation adjacent to the crack surface which always accompanies fracture. It can be shown[8] that both these conditions are satisfied when $K_I \geqslant K_c$, and that

$$K_I = (EG_I)^{\frac{1}{2}}, \qquad (2)$$

for plane stress. For plane strain E is replaced by $E/(1 - \nu^2)$.

K_c and G_c are similarly related and are therefore equivalent measures of fracture toughness.

This equation is sometimes written

$$K_I = \left(\frac{EG_I}{\pi}\right)^{\frac{1}{2}} \tag{3}$$

with the result that all other equations involving K_I differ by a factor $(\pi)^{\frac{1}{2}}$. This variation has caused some confusion in the literature. The form shown in equation (2) is more generally used and is adopted in this report.

4. CRACK DIRECTION

For an isotropic material a crack usually tends to grow in the opening mode and the favourable initial direction of crack growth is often stated[9,10] to be perpendicular to the maximum principal tensile stress. More strictly[11] it is along a plane intersecting the crack tip and perpendicular to the greatest local tensile stress. This plane is often approximately the same as the one perpendicular to the maximum principal tensile stress in an uncracked specimen. For the two-dimensional case the direction of initial crack growth is along a principal stress trajectory whose direction is given by[9,11]

$$K_I \sin\theta = K_{II}(3\cos\theta - 1). \tag{4}$$

If mode III displacements are present a preferred plane for crack growth will intersect the crack front at only one point, so that initially the crack is constrained to a less favourable path although the crack surface may be stepped[12]. If permitted by the specimen geometry, the crack will twist to a favourable path as it grows. The situation may be summarized by stating that whenever possible a crack in a brittle isotropic material grows in mode I.

5. EFFECT OF YIELDING

An uncracked metal plate loaded in uniaxial tension is in a state of plane stress. The insertion of a crack does not affect the plate remote from the crack tip, which remains in plane stress, but the highly stressed material near the crack tip is prevented from contracting in the thickness direction by the material further away from the crack, and is therefore in a state of plane strain. In the interior of the plate there is a transverse stress $\sigma_z = \nu(\sigma_x + \sigma_y)$ where ν is Poisson's ratio. All the plate surfaces, however, will still be in a state of plane stress.

In a metal the yield stress is exceeded near the crack tip and a plastic zone develops; the approximate extent of this plastic zone can be estimated by substituting a yield criterion into the stress field equation. If the plastic zone is small compared with the plate thickness, transverse yielding is restricted and conditions near the crack tip still approximate to plane strain through most of the plate thickness. In fracture mechanics this localized plane strain situation is called plane ~~stress~~ strain[13], see Fig. 4, and exists in most metals[4], provided that the thickness is at least $2.5(K_I/\sigma_Y)^2$, where σ_Y is the yield stress (usually taken as the 0.2 per cent proof stress). A large plastic zone means that σ_z is not fully developed through the specimen thickness; when the plastic zone size becomes comparable with the thickness, yielding can take place on 45° planes, and the stress state near the crack tip changes to plane stress. This happens when the thickness $<<2.5(K_I/\sigma_Y)^2$ and in fracture mechanics is referred to as plane stress.

The actual size and shape of the plastic zone depends on the plastic flow properties of the material[4], but it is proportional to $(K_I/\sigma_Y)^2$. The relaxation of stresses, caused by yielding inside the plastic zone means that to maintain equilibrium the stresses outside the plastic zone must increase slightly. The plastic zone thus increases the effective length of the crack. This effective increase called r_p (a symbol for nominal plastic zone radius) is given approximately by

$$r_p = \frac{1}{2\pi}\left(\frac{K_I}{\sigma_Y}\right)^2 \quad \text{for plane stress} \tag{5}$$

and

$$r_p = \frac{1}{6\pi}\left(\frac{K_I}{\sigma_Y}\right)^2 \quad \text{for plane strain} \tag{6}$$

and is about half the extent of the plastic zone. These corrections are only applicable when the plastic zone is small compared with specimen dimensions in the plane of the plate, and are therefore within the region where the stresses are reasonably accurately described by the stress intensity factor. If the plastic zone becomes too large, which happens when the net section stress exceeds about $0.8\sigma_Y$[6], linear elastic fracture mechanics is no longer applicable. It is not always possible to define the net section stress unambiguously and other criteria may be adopted[4]; for example, that the crack length is at least $2.5(K_I/\sigma_Y)^2$.

The value of K_c is normally a minimum under plane strain conditions, as shown schematically in Fig. 5; it becomes a material property, denoted K_{Ic}, in the same sense as the 0.2 per cent proof stress. The existence of K_{Ic} as a material property is the main justification for the application of linear elastic fracture mechanics to brittle fracture problems.

When a specimen containing a crack is loaded, the crack tip opens without extension of the crack. This movement is called the crack opening displacement and is associated with the development of the plastic zone. Its critical value δ_c when the crack starts to grow is roughly constant[14,15] and approximately equals G_c/σ_Y; δ_c is used as a measure of toughness for low strength steels and has the advantage that it still has meaning at and beyond general yield.

The shear lips[16] which develop at specimen surfaces (Figs 2a and 5) are a result of plastic flow. Shear fracture is associated with yielding under plane stress conditions, which initially exist only at the plate surfaces, and extends progressively as the crack grows until the full width of the shear lip is reached. Shear lip width is roughly constant for a given material, and under plane stress conditions they meet giving a fully developed shear fracture (Fig. 2B). During development of the shear lips the crack tends to bow forward in the plate interior. Even when there is a fully developed shear fracture there is always an initial portion of square fracture roughly triangular in shape (Fig. 2b). Plane stress does not necessarily produce shear fracture; for example, beryllium and some titanium alloys show square fractures irrespective of the state of stress. When the crack front has a complicated shape only average values, through the thickness, can be calculated for G_I or K_I. Various aspects of yielding at crack tips have been fully discussed by a number of authors[2-4,6,10,14,16-19].

6. *R*-CURVE HYPOTHESIS

It was assumed in Section 3 that G_c (and K_c) are independent of crack length so that behaviour is of the type shown in Fig. 6, where instability under rising load conditions occurs when a line (which may be curved) of G_I against a, at constant load, reaches a value equal to G_c at the initial crack length: the load at instability is the same as the load at the start of crack growth.

It is evident[6,20] from the progressive development of shear lips in a thin specimen that the resistance to crack growth R increases as the crack grows from its initial length as shown schematically by curve A in Fig. 7. Instability occurs when a line of G_I at constant load is a tangent to the R curve, that is $G_I = R$ and $\partial G_I/\partial a = \partial R/\partial a$. It is reasonable to assume that the form of the R curve is independent of the initial crack length. However, if the initial crack length is altered, instability may occur at a different value of G_I (Fig. 7, curve B), thus the value of G_c taken as the value of G_I at instability, depends on the initial crack length.

Under plane strain conditions (thick plates) the R curve tends towards the ideal case shown in Fig. 8 (compare with Fig. 6), where the plane strain G_c (G_{Ic}, equivalent to K_{Ic}) is independent of the initial crack length, but R still increases with G_I, until instability. For some materials

of engineering interest, such as maraging steels, the R-curve tends to be of the type shown in Fig. 7 irrespective of specimen thickness. Intermediate behaviour is sometimes observed (Fig. 9); at longer crack lengths (Fig. 9, curve B) there may be a burst of square fracture in the interior of the specimen which is arrested by the development of shear lips; the burst of fracture is often accompanied by an audible click which is called 'pop-in'.

Once instability is reached subsequent behaviour depends on the relative stiffness of the specimen and the loading arrangements. As the crack grows the stiffness of the specimen is reduced. If the load source is 'soft' (approaches constant (dead) load conditions) the displacement will increase automatically to compensate for the loss of stiffness without decrease of load and the crack will extend catastrophically. When the load source is sufficiently 'hard' and approaches constant displacement (fixed grip) conditions the loss of stiffness may unload the specimen sufficiently to arrest the crack. Further displacement will be required to extend the crack, and the load will adjust itself so that the R curve is followed[21]. Whether the crack will extend catastrophically when it starts to grow therefore depends on the relative stiffnesses of the specimen and the load source; a large specimen may contain sufficient strain energy to cause complete fracture even under hard loading conditions.

7. DETERMINATION OF K_{Ic} AND PLANE STRESS K_c

The complicated nature of crack growth in metals means that K_{Ic} cannot necessarily be calculated from the load at which instability occurs under plane strain conditions. However, it has been found[22] that consistent values for K_{Ic} are obtained if it is calculated from the load necessary to cause a significant increase in crack length. A significant increase is defined as an increase in effective crack length (actual crack growth plus the apparent growth due to the development of the plastic zone) of 2 per cent, and at least half this must be actual crack growth.

Crack growth can be detected by measuring the displacement across the crack, using a strain-gauged clip gauge[23] (Fig. 10), which is not damaged when the specimen breaks. If a curve of load against displacement is recorded autographically the load used to calculate K_{Ic} can be obtained by a simple geometrical construction (see Appendix III), known as the offset procedure. With lower strength materials the value of K_{Ic} tends to increase and the minimum specimen dimensions necessary to obtain a plane strain fracture, and ensure essentially elastic behaviour, increase rapidly as σ_Y decreases. In practice K_{Ic} can only be conveniently determined if σ_Y is greater than about 100 hbar (65 ton/in^2) for steels and 30 hbar (20 ton/in^2) for aluminium alloys.

To obtain consistent values for K_{Ic} the crack tip radius must be below a certain critical value, which for most metals is less than the sharpest possible machined notch. Specimens are therefore cracked by fatigue loading before testing; the notch from which the crack is grown, and the fatigue loading, must be carefully controlled so that the crack is of the desired form, with a reasonably straight front. To obtain reproducible results the test procedures must be strictly controlled; if test requirements are violated there is usually no means of telling whether the apparent value of K_{Ic} is greater or less than the true value, or of estimating the likely error. Standards describing methods of determining K_{Ic} are being prepared.

Although K_c usually has a more general meaning it is sometimes used to indicate the critical value of K_I under plane stress conditions[6]. A shear fracture (Fig. 2b) is taken to indicate plane stress conditions, and K_c is calculated from the crack length and load at instability. The R curve is usually well rounded (see Section 6) so that the value of the plane stress K_c will depend upon the initial crack length. There is usually some slow crack growth before instability, so that the determination of the actual crack length at instability is difficult[6]. Plane stress K_c testing is less well developed than K_{Ic} testing. K_c values are sometimes measured for intermediate states of stress using the plate thickness which will be used in service.

If a specimen is loaded so that more than one mode of crack surface displacement is present crack growth will start at a critical value of some function of K_I, K_{II} and K_{III}, but will not, in

general, be in the same direction as the original crack (see Section 4). Crack growth will often be stable in the sense that a rising load is needed to cause further growth. For plate bending problems critical values of the plate bending stress intensity factor K_B (see Appendix I) are occasionally quoted.

8. EFFECT OF ANISOTROPY

Elastic anisotropy can usually be ignored in the measurement of K_{Ic} and plane stress K_c (see Appendix IV), provided that crack growth occurs in the original crack plane. In the presence of moderate toughness anisotropy the specimen is simply oriented so that toughness is measured in the direction of interest. Similarly, if toughness varies, for example in the vicinity of a weld, the specimen is cut so that the crack tip is in the required zone. If the toughness anisotropy is marked crack growth will tend to be in the weaker direction, and may not be in the direction of the initial crack even for mode I loading. The testing of a glued joint can be regarded as an extreme case of toughness anisotropy.

When the direction of crack growth is unstable (Appendix I) (Fig. 3e) an artificial plane of weakness is sometimes created by cutting one or two side grooves along the prospective crack plane to ensure that the crack grows in the desired direction. Only an approximate correction[24] is available to allow for the effect of the side grooves on the stress intensity factor.

Values of K_c can be obtained for fibre reinforced materials, provided that the crack extends in its original direction[25]; this will always be the case in the weak direction, but only occurs in the strong direction for less satisfactory composites. In a good composite the crack is diverted parallel to the fibres and a complex crack pattern appears which increases the toughness. No mathematical solution is available for this situation, so that at present the toughness of fibre reinforced materials cannot be satisfactorily assessed using fracture mechanics techniques.

9. EFFECT OF STRAIN RATE

The stress intensity factor concept can be applied to moving cracks (see Appendix V) and can therefore be applied to the examination of the behaviour of a propagating crack. When K_I exceeds K_c a crack will start to grow, and will continue to grow provided that K_I is at least equal to K_c. Any energy in excess of that required to form new crack surfaces causes the crack growth rate to accelerate towards a theoretical limit; as this is approached surplus energy causes crack branching and, possibly, shattering. If K_c increases with crack speed the crack speed adjusts itself so that $K_c = K_I$.

Provided the rate of increase of K_I, $\dot{K}$, is known, the strain rate for any point near the crack tip can be calculated using equation (1.1) of Appendix I. Similarly, the strain rate can be calculated for a propagating crack from the value of K_I and the crack speed. Increase of both $\dot{K}$ and crack speed cause an increase in strain rate near the crack tip, but there is no simple relationship between the two. The situation is further complicated by the presence of a plastic zone, and for some purposes it is convenient to compare stress rates[13] (rate of increase of stress) rather than strain rates. The stress rate is a maximum at the leading edge of the plastic zone. For plane stress the maximum stress rate S at a stationary crack with constant rate of load increase is given by

$$S = \frac{2\sigma_Y}{t}, \tag{7}$$

t = time from zero load.

For a crack propagating at velocity V and under plane stress conditions S is given by

$$S = \frac{\sigma_Y V}{2r_p}, \tag{8}$$

where r_p is given by equation (5).

If the material is strain rate sensitive the problem is further complicated by the increase in σ_Y at high strain rates, because the value of σ_Y is itself a function of S.

Most high strength materials are not particularly strain rate dependent so that K_c is only slightly affected by the value of S. Mild and similar steels are markedly strain rate sensitive, and crack initiation is more difficult than crack propagation[13,26], particularly above the transition temperature. The relationship between K_c and S, above the transition temperature, is shown schematically in Fig. 11. At low loading rates mild steel is too tough to obtain a value for K_c using specimens of practical size, but if a crack is initiated by any means it will accelerate rapidly towards the crack speed associated with the minimum K_c and is not readily arrested. The decrease in K_c at high loading rates with the associated increase in σ_Y means that much smaller specimens will behave in an essentially elastic manner[27], and explains the importance of impact loads as a cause of brittle fractures. The K_c required to initiate a crack can also be considerably reduced by metallurgical damage, perhaps associated with welding, and by local cooling.

10. FATIGUE CRACK GROWTH

The previous sections were concentrated on the application of linear elastic fracture mechanics to brittle fracture. However, the concept of stress intensity factor can be used in the study of mechanisms[28] such as fatigue and stress corrosion, which cause slow crack growth at stress intensity factors below K_c, and are sometimes referred to as 'sub-critical crack growth'.

Numerous, apparently different, 'laws' of fatigue crack growth have been described in the literature[29], and by making various plausible assumptions some of them can be derived theoretically. All the laws can be regarded as valid in the sense that they describe a particular set of fatigue crack growth data, and they can be used to predict crack growth rates in situations similar to those used to collect the data. It is sometimes possible to fit the same set of data to apparently contradictory laws, but owing to the inherent scatter in fatigue crack growth data it is not possible to decide which law is the most 'correct'.

Linear elastic fracture mechanics provides a particularly convenient means of correlating fatigue crack growth data[30] because the stress conditions at the crack tip can be described by a single parameter, the stress intensity factor. Apart from the development of shear lips and tilting of cracks onto a shear plane, sometimes observed in thin sheets, fatigue crack growth normally occurs[31] in mode I, and its direction is therefore as described in Section 4. The fatigue cycle is usually described by ΔK ($K_{max} - K_{min}$, where K_{max} and K_{min} are the maximum and minimum values of K_I during the fatigue cycle). It has been shown experimentally that ΔK has the major influence on fatigue crack growth[30] and that if ΔK is constant the fatigue crack growth rate is constant[32]. For many materials where the fatigue cycle is entirely tensile the rate of fatigue crack growth can be expressed by the equation

$$da/dN = C(\Delta K)^m \qquad (9)$$

where N is number of cycles, C a material constant, and m is an exponent usually about 4.

Equation (9) is sometimes modified to allow for the increase in crack growth rate which usually occurs as K_{max} approaches K_c, and for the effect of mean stress, which influences fatigue crack growth rate in some materials. If ΔK is below a certain threshold value fatigue crack growth does not occur[28,33].

Equation (9) applies only to an essentially elastic situation, so that limitations of the type described in Section 5 should be applied to K_{max}; corrections to K_{max} may be made for plastic zone size using equation (5) or (6). Corrections to ΔK may be made for plastic zone sizes using these equations, but σ_Y is replaced by $2\sigma_Y$[17]. The resulting correction to ΔK is usually very small and is normally neglected. The minimum value of K_I (K_{min}) during the fatigue cycle equals $K_{max} - \Delta K$. For the case of a zero minimum load K_{min} would be expected to be zero, but if

plastic zone corrections are applied $K_{max} > \Delta K$, and K_{min} has a small positive value: the crack is effectively held open by the plastic zone, so that a small compressive load is required to close the crack and reduce K_{min} to zero. For an alternating load it is conventional to calculate ΔK on the assumption that the crack is completely closed on the compressive half cycle so that the effective load cycle is zero to maximum load. The effect of the plastic zone is to increase ΔK somewhat because the crack is actually open during part of the compressive half cycle; the effect is more marked for short crack lengths. When a crack has grown for some distance the permanent deformation adjacent to the crack surface, left behind by the passage of the plastic zone at the crack tip, may be sufficient to cause closure of the crack before the load has fallen to zero[34], thus reducing ΔK.

When a centre crack specimen (Fig. 3c) is used K_{max} and ΔK both increase with crack length, but the stress ratio R remains constant; data are usually presented as plots of da/dN against ΔK for constant R. Constant K specimens where K_I is independent of crack length (Fig. 3e) are particularly convenient because all the parameters can easily be varied independently. Note that plotting data by different methods, for example, da/dN against ΔK for constant K_{mean} instead of constant R, can give a different impression of the fatigue crack growth properties of a material.

If the maximum fatigue load is such that general yielding occurs it may still be possible to apply linear elastic fracture mechanics, provided the alternating load is small. In this case it can be argued that the unloading displacements during the first cycle, and all the subsequent cycles, will be essentially elastic so that it is possible to calculate ΔK, although K_{max} cannot be calculated. This argument has been found[33] to be justified for some materials because equation (9) has been found to be applicable beyond general yielding.

11. STRESS CORROSION CRACKING

In a conventional stress corrosion test a plain specimen is loaded to near its yield point and left to break. Most of the time to failure is occupied by the development of corrosion pits which eventually lead to cracking and failure. The test is thus primarily a test of resistance to pitting, and not of the ability of a cracked material to resist crack extension in the presence of a corrosive. In-service, cracks may be present, so information on the stress corrosion resistance in the presence of a crack[35] is required. This is particularly important for materials such as titanium alloys, which are resistant to pitting but may be sensitive to stress corrosion in the presence of a crack[36].

In these circumstances a fracture mechanics approach can be used. Cracked specimens can be loaded to various values of K_I and the stress corrosion crack growth rate determined. It is found that there is a threshold value[28,35,36] of K_I (K_{ISCC}) below which no crack growth occurs; K_{ISCC} is a useful index of a materials stress corrosion resistance. For satisfactory results specimens should be of such a size that behaviour is essentially elastic and plane strain conditions exist (see Sections 5 and 7).

12. APPLICATIONS

In the past the problem of brittle fracture was tackled by empirical methods based on service experience, and a great many tests were devised, the best known of which is the Charpy impact test. Until the advent of fracture mechanics there was no really satisfactory method of assessing the fracture toughness of high-strength materials (say, greater than 100 hbar (65 ton/in^2) for steels and 30 hbar (20 ton/in^2) for aluminium alloys), but the determination of K_{Ic} is now an established method of assessing such materials[37].

Methods of measuring toughness are needed for the development of new materials, for quality control during material production, and to provide design information. The determination of K_{Ic} is now being used for material development, and its use is being planned for quality control and specification purposes. One particular value of K_{Ic} is that it can readily be used to measure the toughness at any area of interest, for example, at or near welds, by suitable orientation of the test specimen and positioning of the initial crack.

In principle application to design problems is straightforward[38,39]. The relationship between K_{Ic}, applied stress σ, and initial flaw size a at the start of crack growth can be written in the general form

$$K_{Ic} = \sigma(\pi a)^{1/2}\alpha, \tag{10}$$

where α is a correction factor for the geometry of the flaw and structure. The determination of stress intensity factors for various geometries is described briefly in Appendix VI. Thus, if any two factors (that is, flaw size, applied stress or K_{Ic}) are known, it is then possible to determine the value of the third to avoid brittle fracture. The plastic zone increases the effective flaw size, and a correction should be included if it is a significant proportion of the flaw size. Equation (10) only holds under essentially elastic conditions (see Sections 5 and 7) where failure occurs at below general yield. If the material is too thin for fully developed plane strain conditions (Fig. 5) K_{Ic} in equation (10) is replaced by the value of K_c appropriate to the thickness.

If the flaw is too small to cause a brittle fracture it may nevertheless be above the threshold size (see Sections 10 and 11) for stress corrosion or fatigue crack growth. In this case the time required for the flaw to grow to a critical size can be obtained from appropriate crack growth data and be used to estimate the safe life of the component.

In practice there are considerable difficulties in applying this approach. First, accurate values of α in equation (10) for three-dimensional bodies are only available for a few simple crack shapes in regular bodies; at present this is the biggest obstacle to a more widespread application of fracture mechanics in design. Secondly, the loadings on the structure may not be sufficiently known for accurate estimates of stress level to be made. Thirdly, flaw size often cannot be accurately determined using the available non-destructive testing techniques and lastly, there may be considerable scatter in the toughness of a material, particularly in the vicinity of welds. Despite these shortcomings fracture mechanics has been successfully applied to a number of design problems, especially in the aerospace industry, and has proved particularly valuable in failure analysis.

Many of the difficulties associated with the analytic approach outlined above can be avoided by proof testing[38,39]. If the structure does not fail, and K_{Ic} is known, the stress intensity factor at the tip of the worst flaw cannot exceed K_{Ic} at the proof load, and on this basis it is sometimes possible to make realistic calculation on the rate of growth of cracks during the service life of the structure. This approach has been applied to pressure vessel design.

13. CONCLUSIONS

(1) The crack tip stress field in an essentially elastic situation, that is below general yield, can be described by the stress intensity factor, which has the dimensions of (stress) × (length)$^{1/2}$. The stress intensity factor should not be confused with either a stress concentration factor or a stress intensification factor. Two alternative definitions of stress intensity factor exist: these differ numerically by a factor of $\pi^{1/2}$.

(2) Crack growth under static loading starts when the stress intensity factor reaches a critical value; under plane strain conditions this is a minimum denoted K_{Ic}, which can be regarded as a material property in the same sense as the 0.2 per cent proof stress, and is a convenient measure of a material's fracture toughness, or resistance to brittle fracture. The determination of K_{Ic} involves careful experimental work; published values should be regarded with suspicion unless it is known that the test technique is adequate.

(3) The concept of stress intensity factor can also be used in the analysis of stress corrosion and fatigue crack growth data. In both cases it is found that there is a threshold below which crack growth does not occur.

(4) The high stresses at a crack tip lead, in metals, to the development of a plastic zone, which increases the effective length of a crack. In accurate work it is sometimes necessary to make a correction for the plastic zone.

(5) The concept of stress intensity factor can be applied to problems in design and failure analysis provided that general yielding does not occur. A serious limitation is a lack of information on stress intensity factors for irregular cracks in complex three-dimensional shapes.

REFERENCES

1. LIEBOWITZ, H. (Ed.) *Fracture - an advanced treatise.* New York: Academic Press, 1968-70.

2. PARIS, P. C. and SIH, G. C. Stress analysis of cracks. *Symp. on Fracture Toughness Testing and its Applications. ASTM STP*, 381, pp 30-83. Philadelphia, Pa.: American Society for Testing and Materials, 1965.

3. BILBY, B. A. and SWINDEN, K. H. Representation of plasticity at notches by linear dislocation alloys. *Proc. R. Soc. A.*, 1965, **285**(1400), 22-33.

4. BROWN, W. F. and SRAWLEY, J. E. Plane strain crack toughness testing of high strength metallic materials. *ASTM STP*, 410. Philadelphia, Pa.: American Society for Testing and Materials, 1966.

5. MOSTOVOY, S., CROSSLEY, P. B. and RIPLING, E. J. Use of crack line loaded specimens for measuring plane strain fracture toughness. *J. Mater.*, 1967, 2(3), 661-681.

6. SRAWLEY, J. E. and BROWN, W. F. Fracture toughness testing. *Symp. on Fracture Toughness Testing and its Applications, ASTM STP*, 381, pp 133-198. Philadelphia, Pa.: American Society for Testing and Materials, 1965.

7. COTTRELL, A. H. *The mechanical properties of matter.* New York: John Wiley, 1964.

8. IRWIN, G. R. Analysis of stresses and strains near the end of a crack traversing a plate. *J. appl. Mech.*, 1957, **24**, 361-364.

9. COTTEREI L, B. Notes on the paths and stability of cracks. *Int. J. fracture Mech.*, 1966, 2(3), 526-533.

10. CHEREPANOV, G. P. Cracks in solids. *Int. J. Solids & Struct.*, 1968, 4(8), 811-831.

11. ERDOGAN, F. and SIH, G. C. On the crack extension in plates under plane loading and transverse shear. *J. bas. Engng*, 1963, **85**(4), 519-527.

12. POOK, L. P. The effect of crack angle on fracture toughness. *NEL Report* No 449. East Kilbride, Glasgow: National Engineering Laboratory, 1970.

13. KENNY, P. and CAMPBELL, J. D. Fracture toughness - an examination of the concept in predicting the failure of materials. *Prog. Mater. Sci.*, 1967, 13(3), 135-181.

14. WELLS, A. A. Notched bar tests, fracture mechanics and the brittle strengths of welded structures. *Houdrement Lecture*, 1964. *Weld. in Wld - Soundage dans le Monde*, 1964, 2(4), 198-219, or *Br. Weld J.*, 1965, 12(1), 2-13.

15. DOBSON, M. O. (Ed.) *Practical fracture mechanics for structural steels.* London: Chapman & Hall, 1969.

16. HAHN, G. T. and ROSENFIELD, A. R. Sources of fracture toughness: the relation between K_{Ic} and the ordinary tensile properties of metals. Applications related phenomena in titanium alloys. *ASTM STP*, 432, pp 5-32. Philadelphia, Pa.: American Society for Testing and Materials, 1968.

17. RICE, J. R. Mechanics of crack tip deformation and extension by fatigue. Fatigue crack growth. *ASTM STP*, 415, pp 247-309. Philadelphia, Pa.: American Society for Testing and Materials, 1967.

18. BARENBLATT, G. I. Mathematical theory of equilibrium cracks in brittle fracture. *Adv. appl. Mech.*, 1961, **7**, 55-129.

19. DIXON, J. R. Stress and strain distributions around cracks in sheet materials having various work-hardening characteristics. *Int. J. fracture Mech.*, 1965, **1**(3), 224-244.

20. CLAUSING, D. P. Crack stability in linear elastic fracture mechanics. *Int. J. fracture Mech.*, 1969, **5**(3), 211-227.

21. SWANSON, S. R. The validity of fracture toughness data as influenced by test machine response. *Conf. on Fracture Toughness Theory and Practice*, I.S.I. Publ. 120. London: Iron and Steel Institute, 1970.

22. SRAWLEY, J. E., JONES, M. H. and BROWN, W. F. Determination of plane strain fracture toughness. *Mater. Res. & Stand.*, 1967, **7**(6), 262-266.

23. FISHER, D. M., BUBSEY, R. T. and SRAWLEY, J. E. Design and use of displacement gage for crack-extension measurements. *NASA TN* D-3724. Washington, D.C.: National Aeronautics and Space Administration, 1966.

24. FREED, C. N. and KRAFFT, J. M. Effect of side grooving on measurement of plane strain fracture toughness. *J. Mater.*, 1966, **1**(4), 770-790.

25. BAKER, A. A. and CRATCHLEY, D. Stress-strain behaviour and toughness of a fibre-reinforced metal. *Appl. Mater. Res.*, 1966, **5**(2), 92-103.

26. DVORAK, J. and VRTEL, J. Measurement of fracture toughness in low-alloy mild steels. The Griffith-Irwin theory is applied to fracture of nitrided mild steel specimens. *Weld. J. Res. Suppl.*, 1966, **45**(6), 272s-283s.

27. RADON, J. C. and TURNER, C. E. Note on the relevance of linear fracture mechanics to mild steel. *J. Iron Steel Inst.*, 1966, **204**(8), 842-845.

28. JOHNSON, H. H. and PARIS, P. C. Sub-critical flaw growth. *Engng fracture Mech.*, 1968, **1**(1), 1-45.

29. CHRISTENSEN, R. H. and HARMON, R. B. Limitation of fatigue crack research in the design of flight vehicle structures. Fatigue crack growth. *ASTM STP*, 415, pp 5-24. Philadelphia, Pa.: American Society for Testing and Materials, 1967.

30. PARIS, P. C. and ERDOGAN, F. A critical analysis of crack propagation laws. *J. bas. Engng*, 1963, **85**(4), 528-534.

31. IIDA, S. and KOBAYASHI, A. S. Crack-propagation rate in 7075-76 plates under cyclic tensile and transverse shear loadings. *J. bas. Engng*, 1969, **91D**(4), 764-769.

32. SWANSON, S. R., CICCI, F. and HOPPE, W. Crack propagation in clad 7079-T6 aluminium alloy sheet under constant and random amplitude fatigue loading. Fatigue crack growth. *ASTM STP*, 415, pp 312-360. Philadelphia, Pa.: American Society for Testing and Materials, 1967.

33. FROST, N. E., POOK, L. P. and DENTON, K. A fracture mechanics analysis of fatigue crack growth data for various materials. *Engng fracture Mech.*, (to be published).

34. ELBER, W. Effect of the plastic zone on the crack propagation under cyclic loads (in German). *Materialprufung*, 1970, **12**(6), 189-193.

35. BEACHEM, C. D. and BROWN, B. F. A comparison of three pre-cracked specimens for evaluating the susceptibility of high-strength steel to stress corrosion cracking. Stress corrosion testing. *ASTM STP*, 425, pp 31-40. Philadelphia, Pa.: American Society for Testing and Materials, 1967.

36. LANE, I. R. and CAVALLARO, J. L. Metallurgical and mechanical aspects of the sea-water stress corrosion of titanium. Applications related phenomena in titanium alloys. *ASTM STP*, 432, pp 147-169. Philadelphia, Pa.: American Society for Testing and Materials, 1968.

37. IRON AND STEEL INSTITUTE. Fracture toughness. *ISI Publ.* No 121. London: Iron and Steel Institute, 1969.

38. TIFFANY, C. F. and MASTERS, J. N. Applied fracture mechanics. *Symp. on Fracture Toughness Testing and its Applications, ASTM STP*, 381, pp 249-277. Philadelphia, Pa.: American Society for Testing and Materials, 1965.

39. COLLIPRIEST, J. E. and KIZER, D. E. Experimental verification of proof-test logic. *Metals Eng. Q.*, 1969, **9**(4), 43-48.

40. SIH, G. C., PARIS, P. C. and ERDOGAN, F. Crack tip stress intensity factors for plane extension and plate bending problems. *J. appl. Mech.*, 1962, **29**(2), 306-312.

41. JAHSMAN, W. E. and FIELD, F. A. The effect of residual stresses on the critical length predicted by the Griffith theory. *J. appl. Mech.*, 1963, **30**(4), 613-616.

42. POOK, L. P. Effect of hardness and tensile mean stress on fatigue crack growth in beryllium copper. *J. mech. Engng Sci.*, 1969, **11**(3), 343-345.

43. LARSON, F. R. Anisotropy of titanium sheet in uniaxial tension. *Trans. Am. Soc. Metals*, 1964, **57**(3), 620-631.

44. SIH, G. C., PARIS, P. C. and IRWIN, G. R. On cracks in rectilinearly anisotropic bodies. *Int. J. fracture Mech.*, 1965, **1**(3), 189-203.

45. WU, E. M. Application of fracture mechanics to orthotropic plates. *J. appl. Mech.*, 1967, **34**(4), 967-974.

46. COTTEREI L, B. Fracture propagation in organic glasses. *Int. J. fracture Mech.*, 1968 **4**(3), 209-217.

47. TIMOSHENKO, S. *Theory of elasticity.* New York: McGraw-Hill, 1934.

48. HARRIS, D. O. Stress intensity factors for hollow circumferentially notched round bars. *J. bas. Engng*, 1967, **89D**(1), 49-54.

49. CREAGER, M. and PARIS, P. C. Elastic field equations for blunt cracks with reference to stress corrosion cracking. *Int. J. fracture Mech.*, 1967, **3**(4), 247-252.

50. DIXON, J. R. and POOK, L. P. Stress intensity factors calculated generally using the finite element technique. *Nature*, 1969, **224**(5215), 166-167.

51. KHOL, R. Computer stress analysis. *Mach. Des.*, 1968, **40**(27), 136-145.

52. WILLIAMS, J. G. and ISHERWOOD, D. P. The calculation of the strain energy release rates of cracked plates by an approximate method. *J. strain Anal.*, 1968, **3**(1), 17-22.

53. LAZZERI, L. and PARRY, G. W. *An approximate method of plane strain fracture toughness (K_{Ic}) calculation for notched specimens, ISI Publ.* 120. London: Iron and Steel Institute, 1970.

54. SHAH, R. C. and KOBAYASHI, A. S. On the parabolic crack in an elastic solid. *Engng fracture Mech.*, 1968, **1**(2), 309-325.

55. WESTMANN, R. A. Note on estimating critical stress for irregularly shaped plane cracks. *Int. J. fracture Mech.*, 1966, **2**(3), 561-563.

56. FOLIAS, E. S. On the effect of initial curvature on cracked flat sheets. *Int. J. fracture Mech.*, 1969, **5**(4), 327-346.

LIST OF TABLES

LIST OF FIGURES

9. *R*-curve for 'pop-in' behaviour

10. ASTM-type strain gauged clip gauge mounted on knife edges

11. Relationship for low strength steels between maximum stress rate and K_{Ic}

12. Polar coordinates for crack tip stress field

13. Types of load displacement record illustrating offset procedure for determination of K_{Ic}.

APPENDIX I

ELASTIC STRESS FIELDS

The elastic stress fields and displacements corresponding to the three modes of crack surface displacement are[2], referring to Fig. 1 for notation (where u,v,w are displacements in the x,y,z directions).

Mode I:

$$\sigma_x = \frac{K_I}{(2\pi r)^{1/2}} \cos\frac{\theta}{2}\left(1 - \sin\frac{\theta}{2}\sin\frac{3\theta}{2}\right)$$

$$\sigma_y = \frac{K_I}{(2\pi r)^{1/2}} \cos\frac{\theta}{2}\left(1 + \sin\frac{\theta}{2}\sin\frac{3\theta}{2}\right)$$

$$\tau_{xy} = \frac{K_I}{(2\pi r)^{1/2}} \sin\frac{\theta}{2}\cos\frac{\theta}{2}\cos\frac{3\theta}{2}$$

$$\sigma_z = \nu(\sigma_x + \sigma_y) \qquad \text{(I.1)}$$

$$\tau_{xz} = \tau_{yz} = 0$$

$$u = \frac{K_I}{G}\left(\frac{r}{2\pi}\right)^{1/2} \cos\frac{\theta}{2}\left(1 - 2\nu + \sin^2\frac{\theta}{2}\right)$$

$$v = \frac{K_I}{G}\left(\frac{r}{2\pi}\right)^{1/2} \sin\frac{\theta}{2}\left(2 - 2\nu - \cos^2\frac{\theta}{2}\right)$$

$$w = 0.$$

Note that the crack opens into a parabola, and that because a crack is regarded as a mathematical 'cut', θ must lie within the range $\pm\pi$.

Mode II:

$$\sigma_x = -\frac{K_{II}}{(2\pi r)^{1/2}} \sin\frac{\theta}{2}\left(2 + \cos\frac{\theta}{2}\cos\frac{3\theta}{2}\right)$$

$$\sigma_y = \frac{K_{II}}{(2\pi r)^{1/2}} \sin\frac{\theta}{2}\cos\frac{\theta}{2}\cos\frac{3\theta}{2}$$

$$\tau_{xy} = \frac{K_{II}}{(2\pi r)^{1/2}} \cos\frac{\theta}{2}\left(1 - \sin\frac{\theta}{2}\sin\frac{3\theta}{2}\right)$$

$$\sigma_z = \nu(\sigma_x + \sigma_y) \qquad \text{(I.2)}$$

$$\tau_{xz} = \tau_{yz} = 0$$

$$u = \frac{K_{II}}{G}\left(\frac{r}{2\pi}\right)^{1/2} \sin\frac{\theta}{2}\left(2 - 2\nu + \cos^2\frac{\theta}{2}\right)$$

$$v = \frac{K_{II}}{G}\left(\frac{r}{2\pi}\right)^{1/2} \cos\frac{\theta}{2}\left(-1 + 2\nu + \sin^2\frac{\theta}{2}\right)$$

$$w = 0.$$

Equations (I.1) and (I.2) are written for plane strain; they can be changed to plane stress by writing $\sigma_z = 0$, and substituting the appropriate value for ν.

Mode III:

$$\tau_{xz} = -\frac{K_{III}}{(2\pi r)^{1/2}} \sin\frac{\theta}{2}$$

$$\tau_{yz} = \frac{K_{III}}{(2\pi r)^{1/2}} \cos\frac{\theta}{2}$$

$$\sigma_x = \sigma_y = \sigma_z = \tau_{xy} = 0 \qquad \text{(I.3)}$$

$$w = \frac{K_{III}}{G}\left(\frac{2r}{\pi}\right)^{1/2} \sin\frac{\theta}{2}$$

$$u = v = 0.$$

Equations (I.1) to (I.3) are for static or slowly moving cracks and were obtained from the series expansion of the stress fields by neglecting higher terms in r. They can be regarded as a good approximation when r is small compared with the other dimensions of the body in the x-y plane and are exact as r tends to zero.

K_I is taken as positive when the crack surfaces move apart. A negative K_I only has meaning if the crack is regarded as a narrow slit because if the crack surfaces are pressed together the crack has no effect on the stress distribution. The signs of K_{II} and K_{III} are a matter of convention, but are generally taken as positive.

For some problems involving the bending of cracked plates it is convenient to determine elastic stress fields in the vicinity of cracks, using plate bending theory[2,40]. The resulting stress fields are described by stress intensity factor K_B (for bending) and K_S (for shear). $K_B = K_I(3+\nu)/(1+\nu)$ and is equivalent (at the plate surface) to K_I; and K_S is equivalent to K_{II}. There is no equivalent to K_{III}.

The elastic stress field can be more accurately represented by including further terms. The first four terms for the opening mode, expressed in polar coordinates (Fig. 12) for compactness, are[9]

$$\sigma_r = \frac{a_1}{4}\left(\frac{2a}{r}\right)^{1/2}\left(5\cos\frac{\theta}{2} - \cos\frac{3\theta}{2}\right) + a_2\cos^2\theta +$$
$$+\frac{a_3}{4}\left(\frac{r}{2a}\right)^{1/2}\left(3\cos\frac{\theta}{2} + 5\cos\frac{5\theta}{2}\right) + \frac{a_4}{2}\left(\frac{r}{2a}\right)\left(\cos\theta + \cos 3\theta\right) + O\left(\frac{r}{2a}\right)^{3/2}$$

$$\sigma_\theta = \frac{a_1}{4}\left(\frac{2a}{r}\right)^{1/2}\left(3\cos\frac{\theta}{2} + \cos\frac{3\theta}{2}\right) + a_2\sin^2\theta +$$
$$+\frac{a_3}{4}\left(\frac{r}{2a}\right)^{1/2}\left(5\cos\frac{\theta}{2} - \cos\frac{5\theta}{2}\right) + 3a_4\left(\frac{r}{2a}\right)\left(\cos\theta - \cos 3\theta\right) + O\left(\frac{r}{2a}\right)^{3/2} \qquad \text{(I.4)}$$

$$\sigma_{r\theta} = \frac{a_1}{4}\left(\frac{2a}{r}\right)^{1/2}\left(\sin\frac{\theta}{2} + \sin\frac{3\theta}{2}\right) - \frac{a_2}{2}\sin 2\theta +$$
$$+\frac{a_3}{4}\left(\frac{r}{2a}\right)^{1/2}\left(\sin\frac{\theta}{2} - \sin\frac{5\theta}{2}\right) + a_4\left(\frac{r}{2a}\right)\left(\sin\theta - 3\sin 3\theta\right) + O\left(\frac{r}{2a}\right)^{3/2}.$$

The coefficients a_1, a_2, a_3, a_4 have the dimensions of stress. Because

$$a_1 = \frac{K_I}{2(\pi a)^{1/2}} \qquad \text{(I.5)}$$

it is equivalent to the opening mode stress intensity factor K_I, this term dominates the stress field near the crack tip and controls crack initiation; the other terms become increasingly important further away from the crack tip. If the coefficient a_2 is positive, as it is for the specimen shown in Fig. 3e, the crack will tend to deviate increasingly from its original path as indicated by the dotted line. For the remaining specimens in Fig. 3, a_2 is negative and the cracks will grow in their original paths. The sign of a_2 can be determined from the isochromatic fringes on a photoelastic model; if they lean forward in the direction of crack growth a_2 is negative and if they lean back it is positive. The terms in a_2 represent stresses parallel to the crack, and crack deviation can be prevented by applying a compressive load parallel to the crack.

Under a constant load a crack which has started to grow will continue to grow provided that K_I increases with the crack length a, that is $\partial K_I/\partial a$ is positive. The value of $\partial K_I/\partial a$ can either be obtained from the expression for stress intensity factor for the specimen concerned or from the equation

$$\frac{\partial K_I}{\partial a} = \left(\frac{\pi}{a}\right)^{1/2} \left(a_3 - \frac{a_1}{2}\right). \tag{I.6}$$

The sign of $\partial K_I/\partial a$ is positive for the specimens in Figs 3a, c, d and f, negative in Fig. 3b and zero in Fig. 3e.

APPENDIX II

EFFECT OF RESIDUAL STRESSES

Non-linear effects due to the presence of small-scale residual stresses can be regarded as occurring within the crack tip stress field, and can therefore be neglected[2]. The general effect[41] of such stresses is to reduce the critical crack length for instability, compared with stress-free material, so that the K_{Ic} of the material will be lowered.

The introduction of a crack into a body containing large-scale residual stresses will relieve the residual stresses originally present on the crack plane. The effect on the crack tip stress field is the same as if stresses, equal in magnitude to the original residual stresses but opposite in sign, were applied to the crack surfaces[14]. The resultant stress intensity factor (which may be called K_R) can be calculated from an appropriate expression for such loads. Crack size and direction will affect the value of K_R; it will be positive for tensile residual stresses, and will be superimposed on any stress intensity factor (K_E) due to external loads.

If K_R is not small compared with K_E, the stress intensity factor at the crack tip will not be given accurately by K_E, so that in the determination of K_{Ic} for materials containing complex residual stress patterns there will be an apparent scatter in the values of K_{Ic}, and anomalies in the results obtained from different sized specimens. These variations should not be confused with scatter due to metallurgical factors or errors caused by the use of specimens of inadequate size. The occurrence of detectable distortion of the specimen when the crack starter notch is machined indicates the presence of residual stresses likely to affect the determination of K_{Ic}. The presence of residual stresses must be allowed for when applying fracture mechanics to design problems, and will also affect stress corrosion crack growth.

Because it is the range of stress intensity factor ΔK which controls fatigue crack growth and the value of K_{mean} (or the mean stress) has only a second order effect on the crack growth rate, large-scale residual stresses can be expected to have little effect on crack growth, unless they cause the crack to close, although small-scale residual stresses have been shown[42] to be a cause of mean stress sensitivity.

APPENDIX III

OFFSET PROCEDURE FOR DETERMINATION OF K_{Ic}

To use the offset procedure[22] a precise autographic record is made of the displacement, across the open end of the crack, against load, as the specimen is loaded to failure. Three possible types of load-displacement record are shown in Fig. 13. A secant is drawn whose slope is about 5 per cent less than that of the tangent OA to the initial part of the record (the actual percentage depends on the specimen type). The load P_s is at the intersection of the secant with the record, and gives the load when the effective crack length has increased by 2 per cent. This effective increase is made up of actual crack growth plus an apparent crack growth which is caused by the development of the plastic zone at the crack tip. To determine whether the actual crack growth is at least 1 per cent of the initial crack length, a horizontal line is drawn to represent a constant load of $0.8\,P_s$; provided that the distance along this line from the tangent OA to the record does not exceed one quarter of the corresponding distance at P_s the minimum 1 per cent has been obtained.

The load P_Q is used to calculate K_{Ic} and is determined as follows.

If the load at every point on the record which precedes P_s is lower than P_s, then $P_Q = P_s$ (case I); if there is a maximum load preceding P_s which exceeds it, then this load is P_Q (cases II and III).

APPENDIX IV

ELASTIC ANISOTROPY

On a macroscopic scale, most structural metals, even those having considerable toughness isotropy, are reasonably isotropic in their elastic properties, and the assumptions made in Section 1 can be regarded as being satisfied.

A few materials, such as some alpha titanium alloys in sheet form[43], show normal anisotropy; elastic properties are isotropic in the plane of the sheet, but are different through the thickness. Except for σ_z, stresses are as given by equations (I.1) and (I.2), and the usual equations for stress intensity factor apply.

In a rectilinearly anisotropic material, the elastic constants vary with direction at any given point, but the directions associated with particular values do not vary from point to point. Anisotropic stress intensity factors for such materials can be obtained by methods similar to those for isotropic materials[2,44], and the elastic stress fields are given by equations similar to equations (I.1) to (I.3). Thus, for example, opening mode stress fields are given by

$$\sigma_x = \frac{K_{Ia}}{(2\pi r)^{1/2}} Re\left[\frac{\mu_1\mu_2}{\mu_1 - \mu_2}\left\{\frac{\mu_2}{(\cos\theta + \mu_2 \sin\theta)^{1/2}} - \frac{\mu_1}{(\cos\theta + \mu_1 \sin\theta)^{1/2}}\right\}\right]$$

$$\sigma_y = \frac{K_{Ia}}{(2\pi r)^{1/2}} Re\left[\frac{1}{\mu_1 - \mu_2}\left\{\frac{\mu_1}{(\cos\theta + \mu_2 \sin\theta)^{1/2}} - \frac{\mu_2}{(\cos\theta + \mu_1 \sin\theta)^{1/2}}\right\}\right] \qquad \text{(IV.1)}$$

$$\tau_{xy} = \frac{K_{Ia}}{(2\pi r)^{1/2}} Re\left[\frac{\mu_1\mu_2}{\mu_1 - \mu_2}\left\{\frac{1}{(\cos\theta + \mu_1 \sin\theta)^{1/2}} - \frac{1}{(\cos\theta + \mu_2 \sin\theta)^{1/2}}\right\}\right] .$$

K_{Ia} is the anisotropic opening mode stress intensity factor and μ_1 and μ_2 are dimensionless elastic constants[2]. For the isotropic case $\mu_1 = \mu_2 = i$ and equations (IV.1) reduce to equations (I.1).

Provided that loads are applied remote from the crack, the anisotropic stress intensity factors are numerically equal to the corresponding isotropic cases. The stresses are still proportional to $r^{-1/2}$, but they are differently distributed about the crack tip. In some situations for loads applied at or near the crack surface, elastic constants enter the equations for stress intensity factor[44], and the isotropic and anisotropic values may differ numerically, so that the isotropic results can only be used as a rough approximation.

The equations for displacements differ from the isotropic case, and the displacement direction depends upon the directional properties of the material so that in the general situation it is no longer possible to associate each stress field mode present with the corresponding mode of crack surface displacement (see Sections 2 and 3). If the material is orthotropic, that is it has three mutually perpendicular planes of symmetry in its elastic properties, and provided that the crack lies in one of these planes, then it becomes possible to associate crack displacement and stress field modes. Some crystals, some fibre-reinforced materials[45], and wood are examples of orthotropic materials. If only one stress field mode of displacement is present, then the crack surface displacements will be entirely in this mode provided that the crack lies in a plane of symmetry.

More generally where the direction of the properties varies from point to point, or where the material is not homogeneous, or where a crack encounters, or lies along, a boundary between materials of different properties, the stresses[2] may no longer be proportional to $r^{-1/2}$ and it is not possible to use isotropic solutions even as an approximation.

APPENDIX V

ELASTIC STRESS FIELDS FOR PROPAGATING CRACKS

There is a theoretical limit[2] to the crack speed in an elastic body (approximately 0.38 of the longitudinal speed of sound in the material), which is based on the rate at which elastic strain energy can travel to the crack tip. The stress fields given by equations (I.1) to (I.3) apply only to static or slowly growing cracks. However, the stress field does not undergo any fundamental change until the limiting velocity is approached so that it is convenient to discuss crack growth as well as crack initiation in terms of stress intensity factors. These may be calculated to a reasonable approximation from the expression derived for the static case, although K_I actually decreases[46] as the crack speed increases.

As the limiting speed is approached stresses are still proportional to $r^{-\frac{1}{2}}$, but the character of the stress field changes: nearly equal tensile stresses exist over a wide arc about the tip, so that there is no clearly defined most favourable direction for crack growth. This encourages crack branching, a feature of some brittle fractures.

APPENDIX VI

DETERMINATION OF STRESS INTENSITY FACTORS

This brief description of some of the available methods is confined to the opening mode; similar methods are used for the other two modes. For two-dimensional cases stress intensity factors can be obtained analytically by the usual methods of stress analysis, and solutions are available for a wide range of shapes and loading conditions, for example, Fig. 3 (a) and (b). A stress function is found which satisfies the biharmonic equation (described in any standard text[47] on strength of materials) and the boundary conditions, while the stress intensity factor is obtained from the stresses at the crack tip. Suitable stress functions are not available for many specimens of practical interest (Fig. 3d) and the collocation method is often used; in this method a stress function which fits the boundary conditions along the crack is modified, using a computer[4], to fit the boundary conditions along the specimen borders at a finite number of points. Provided sufficient points are taken, solutions can be made accurate to less than 1 per cent. Alternatively, again using a computer, complex variable methods may be used where the boundary conditions are satisfied exactly, and the shape of the specimen is defined approximately, using a suitable mapping function expressed in polynomial form[4].

If an internal crack, length 2a, is remote from the specimen borders the stress intensity factor can be obtained from a knowledge of the stresses on the prospective crack plane, with the crack absent, using the Green's function[2]

$$K_I = \frac{1}{(\pi a)^{\frac{1}{2}}} \int_{-a}^{a} \sigma_y(x,0) \left(\frac{a+x}{a-x}\right)^{\frac{1}{2}} dx. \qquad \text{(VI.1)}$$

The stress distribution can be obtained either experimentally or analytically.

If a suitable analytical expression for the stress concentration factor is available (Fig. 3c) the stress intensity factor is given by[2,48,49]

$$K_I = \lim_{\rho \to 0} \frac{\sigma_{max}}{2} (\pi\rho)^{\frac{1}{2}}, \qquad \text{(VI.2)}$$

where σ_{max} is the maximum stress at the notch root and equals σK_T, where σ is the nominal stress at the notch, and K_T is the stress concentration factor. Any approximations involved in the determination of the stress concentration factors are reflected in the resulting stress intensity factors. Provided ρ is small K_I can be obtained directly[49] from a value of σ_{max} for a given value of ρ. Any convenient experimental or mathematical method can be used to obtain σ_{max}.

When a crack in a specimen is extended the compliance λ (reciprocal of stiffness) is increased. If λ is measured experimentally for a range of crack lengths, the strain energy release rate is given by[2]

$$G_I = \frac{P^2}{2B^2} \frac{\partial\lambda}{\partial a} \qquad \text{(VI.3)}$$

where P = load, and B = specimen thickness.

In practice very accurate measurement techniques are required and the experimental method is now normally not used. The stress intensity factor for the constant K specimens (Fig. 3e) was originally obtained using the compliance method and was subsequently checked by collocation. Equation (VI.3) can be used to obtain stress intensity factors by means of a simple finite element computer program[50]. Crack surface displacements[31] or stresses[51] near the crack tip, obtained from finite element computer programs can be substituted into equations (I.1) to (I.3) to obtain stress intensity factors, but a large number of elements are necessary for accurate results.

Various empirical methods of obtaining stress intensity factors have been proposed[52,53] although these can only be regarded as approximations they are often useful in practical problems.

Analysis of three-dimensional cracks presents formidable problems. Available exact solutions for the opening mode in three dimensions are confined[2] to axisymmetrical specimens and to circular, elliptical and parabolic[54] cracks in infinite bodies. The elliptical solution has been adapted for the case of a semi-elliptical surface flaw (Fig. 3f) and is useful in the analysis of service failures where the flaw is small compared with the component dimensions. At present only rough estimates can be made for irregularly shaped cracks[2,55], and where the crack size is comparable with the component dimensions. Progress appears to depend on the development of suitable finite element computer programs.

The analysis of cracked shells presents formidable mathematical difficulties, but steady progress is being made[56].

TABLE 1

Some Customary and SI Units used in Fracture Mechanics

Quantity	Customary units	Equivalent	SI units	Equivalents	Conversion factor	Reciprocal	Comments
Length	inch		metre (m)		*1 in = 0.0254 m (exact value)	39.370	The metre is an SI basic unit
Force	lb		newton (N)		*1 lb = 4.448 22 N	0.224 81	The newton is the primary SI unit of force
Stress	k.s.i.	10^3 lb/in^2	hbar	10^2 bar 10^7 N/m^2	*1 k.s.i. = 0.689 476 hbar	1.4504	1 hbar ≈ 1.02 kg/mm^2
Young's modulus (E)	10^6 lb/in^2		GN/m^2	10^9 N/m^2	10^6 lb/in^2 = 6.894 76 GN/m^2	0.145 04	
Stress intensity factor (K) (K_c) (K_{Ic}) ΔK	k.s.i.(in)$^{1/2}$	10^3 lb/in$^{3/2}$	hbar(cm)$^{1/2}$	MN/m$^{3/2}$ 10^6 N/m$^{3/2}$	1 k.s.i.(in)$^{1/2}$ = 1.0988 hbar(cm)$^{1/2}$	0.910 05	
Strain energy release rate (G) Effective surface energy (G_c)	in lb/in^2	lb/in	kN/m	kJ/m^2 10^3 N/m	1 in lb/in^2 = 0.175 13 kN/m	5.7101	1 kN/m = 10^6 erg/cm^2
Impact energy	ft lb		joule (J)		*1 ft lb = 1.335 82 J	0.737 56	

*These conversion factors are taken from BSI publications;
other factors were derived from these and rounded to five figures

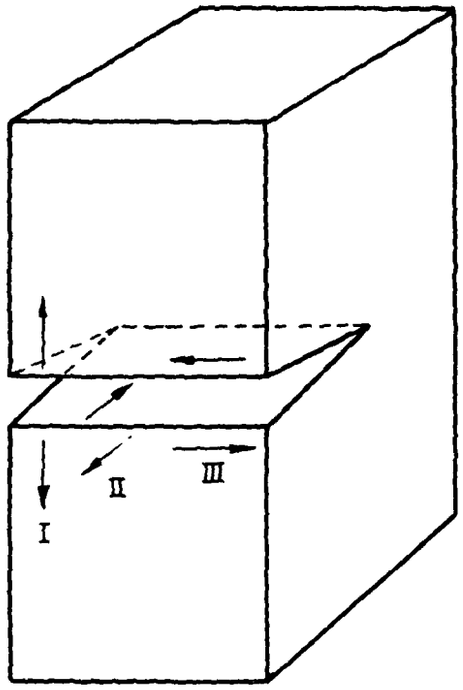

I OPENING MODE

II EDGE SLIDING MODE

III SHEAR MODE

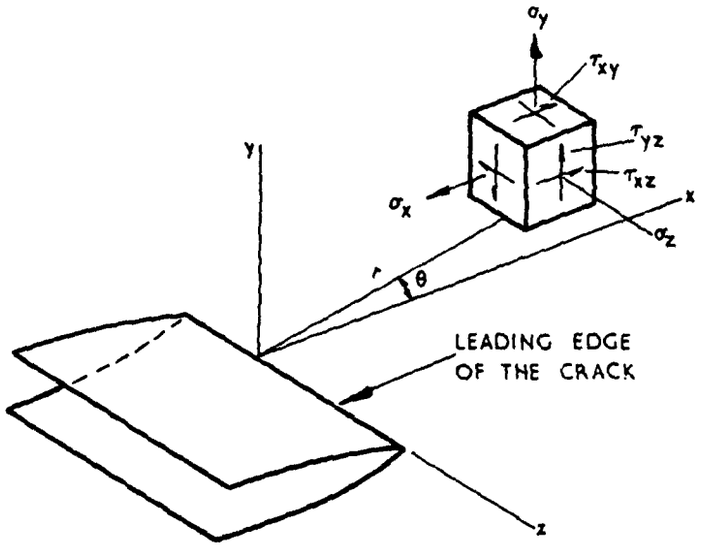

FIG 1 BASIC MODES OF CRACK SURFACE DISPLACEMENT, AND COORDINATES MEASURED FROM THE LEADING EDGE OF A CRACK AND THE STRESS COMPONENTS IN THE CRACK TIP STRESS FIELD (PARIS AND SIH)

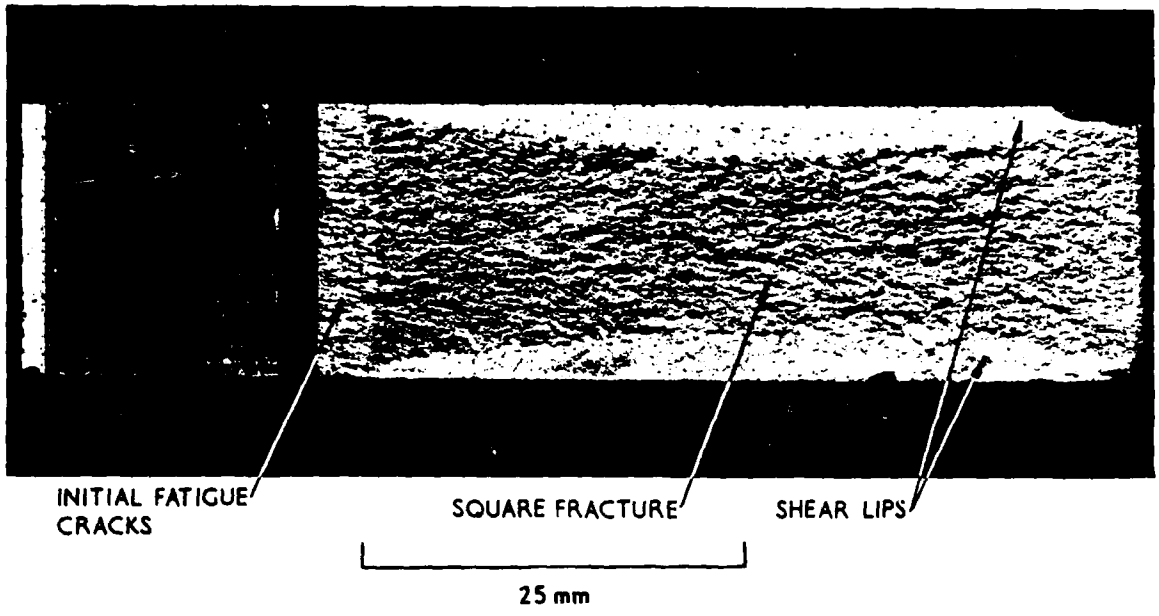

(a) THICK SPECIMEN

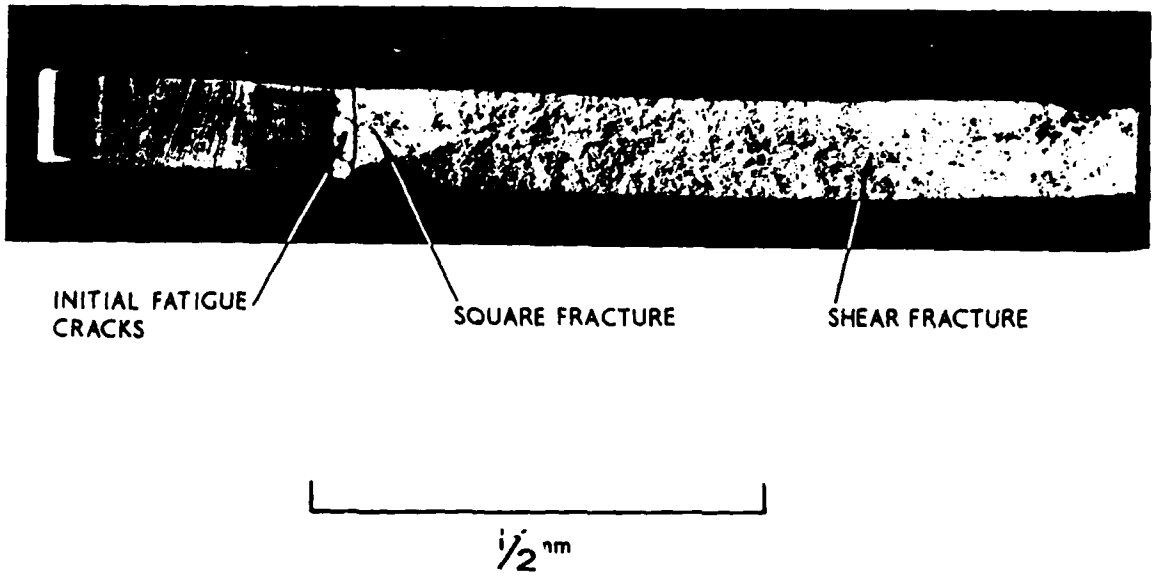

(b) THIN SPECIMEN

FIG 2 FRACTURE SURFACES OF THICK AND THIN SPECIMENS

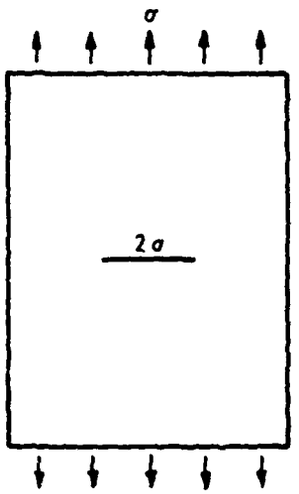

(a) CENTRE CRACK IN INFINITE PLATE. REMOTE LOAD

$K_1 = \sigma (\pi a)^{1/2}$

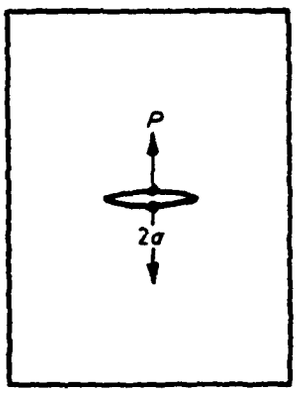

(b) CENTRE CRACK IN INFINITE PLATE. POINT LOADS ON CRACK SURFACES.

$K_1 = \frac{P}{B(\pi a)^{1/2}}$

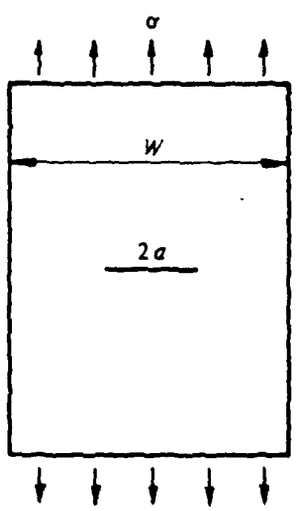

(c) CENTRE CRACK IN PLATE OF FINITE WIDTH REMOTE LOAD.

$Y = K_1/\sigma a^{1/2} = 1{\cdot}77 + 0{\cdot}227(2a/W) - 0{\cdot}510(2a/W)^2 + 2{\cdot}7(2a/W)^3$

$2a/W \leq 0{\cdot}7$

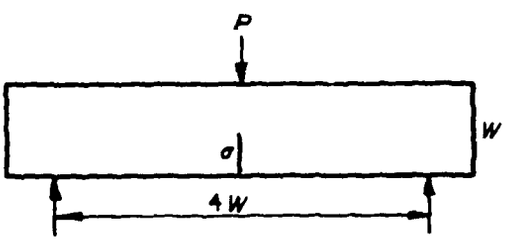

(d) EDGE CRACK PLATE LOADED IN THREE-POINT BEND

$Y = K_1 BW/bPa^{1/2} = 1{\cdot}93 - 3{\cdot}07(a/W) + 14{\cdot}53(a/W)^2 - 25{\cdot}11(a/W)^3 + 25{\cdot}80(a/W)^4$

$a/W \leq 0{\cdot}6$

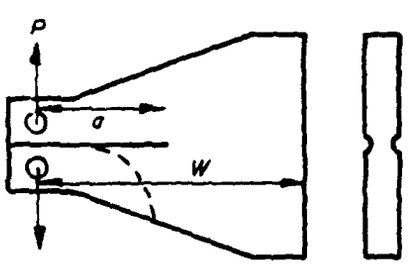

(e) CONSTANT K SPECIMEN

$K_1 B W^{1/2}/P = 10{\cdot}9$

$0{\cdot}2 \leq a/W \leq 0{\cdot}5$

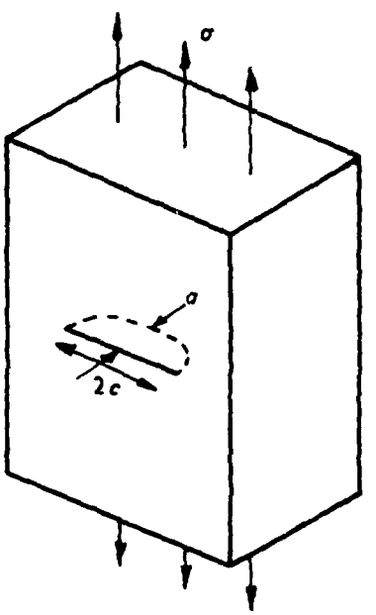

(f) SEMI-ELLIPTICAL CRACK IN SEMI-INFINITE BODY

$K_1 = \frac{1{\cdot}1\sigma(\pi a)^{1/2}}{\phi} \quad \phi = \int_0^{\pi/2} \left[1 - \left(\frac{c^2 - a^2}{c^2}\right)\sin^2\theta\right]^{1/2} d\theta$

FIG 3 STRESS INTENSITY FACTORS FOR VARIOUS CONFIGURATIONS

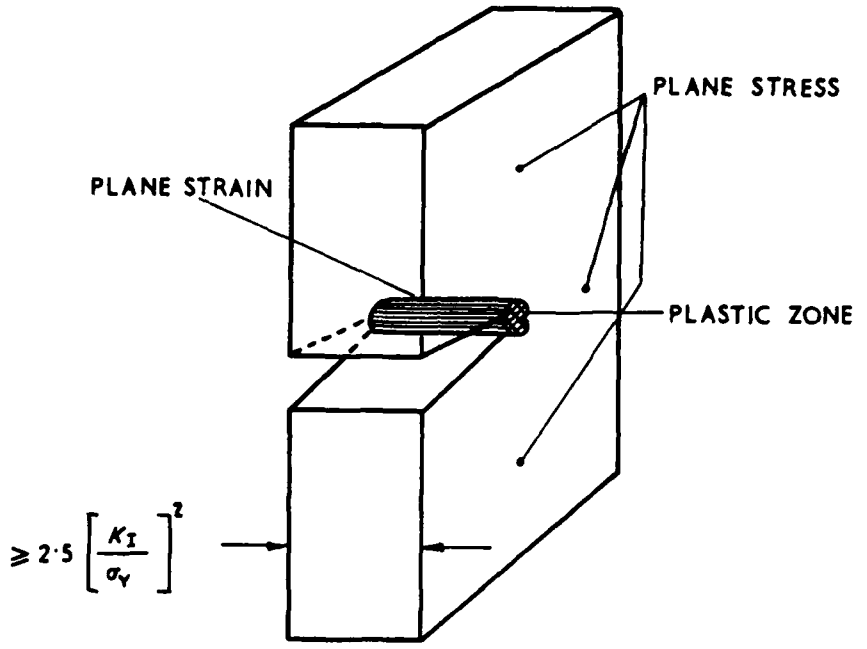

(a) PLANE STRAIN

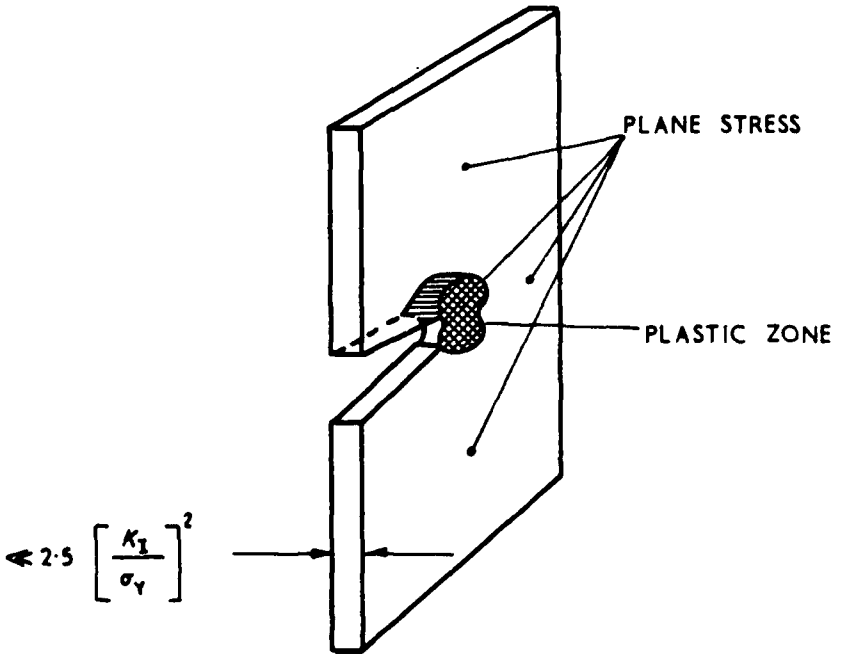

(b) PLANE STRESS

FIG 4 NOMENCLATURE FOR THE STATE OF STRESS IN A CRACKED PLATE

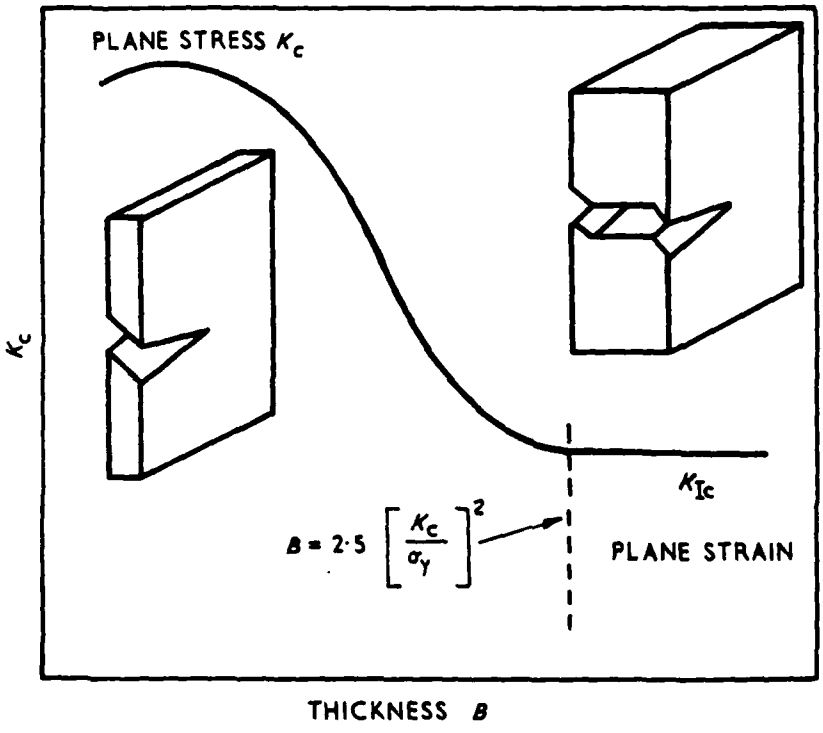

FIG 5 RELATIONSHIP BETWEEN THICKNESS AND K_c

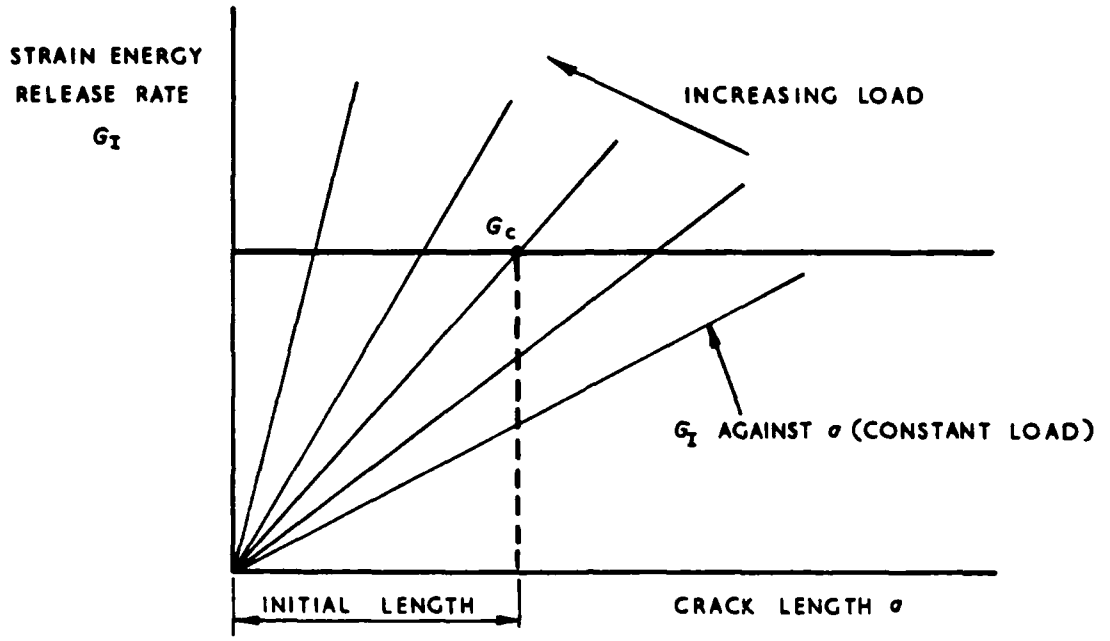

FIG 6 TYPE OF INSTABILITY ORIGINALLY ASSUMED

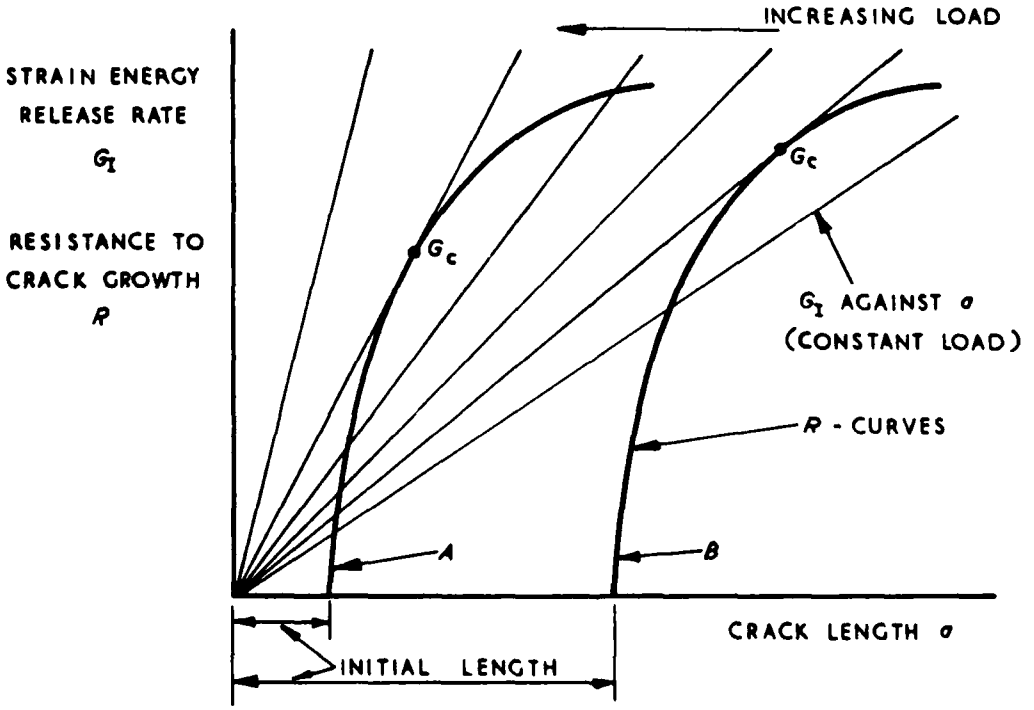

FIG 7 R-CURVE FOR GENERAL CASE

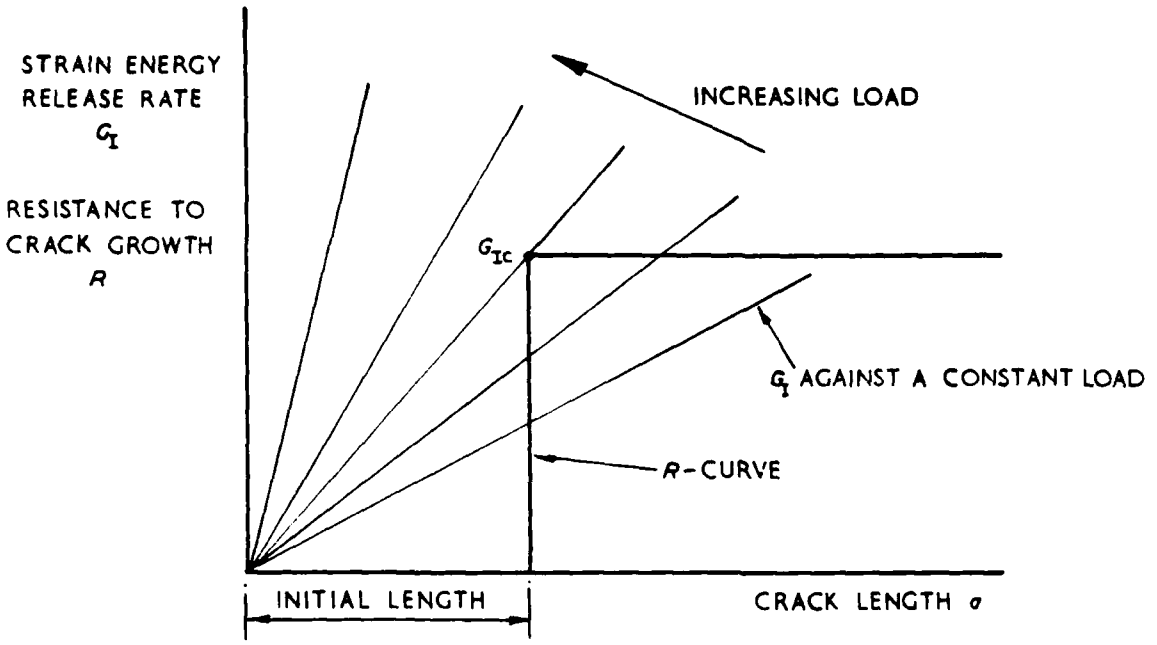

FIG 8 R-CURVE FOR IDEAL BEHAVIOUR

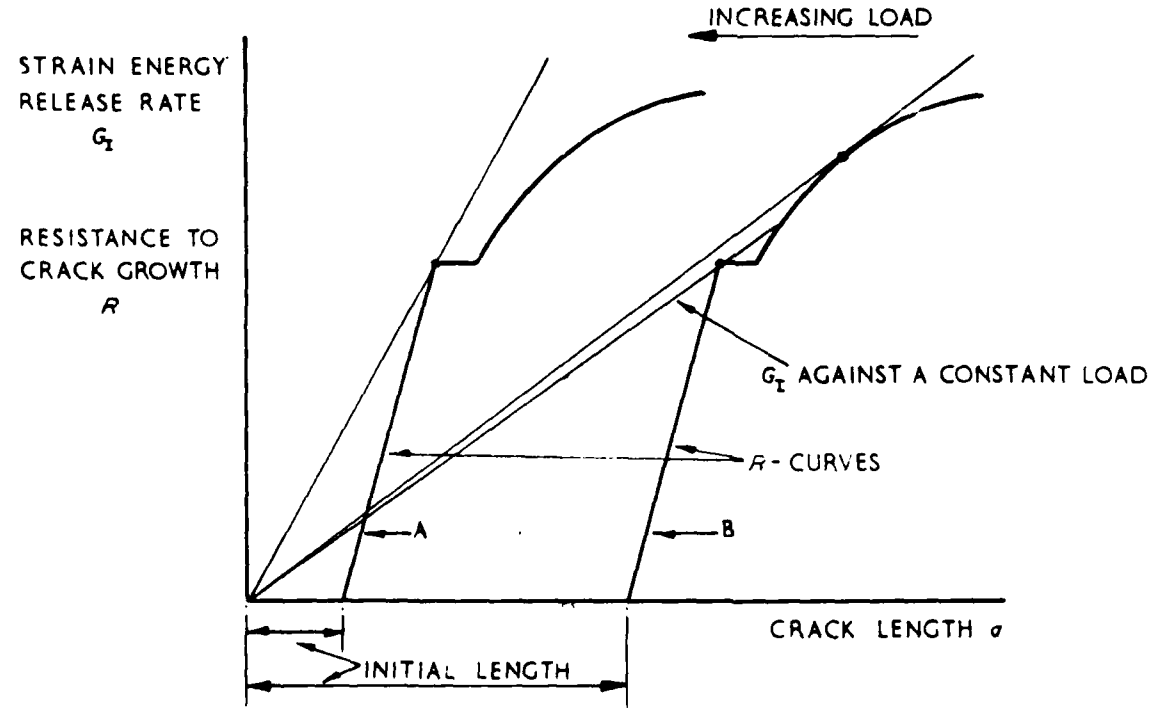

FIG 9 R-CURVE FOR 'POP-IN' BEHAVIOUR

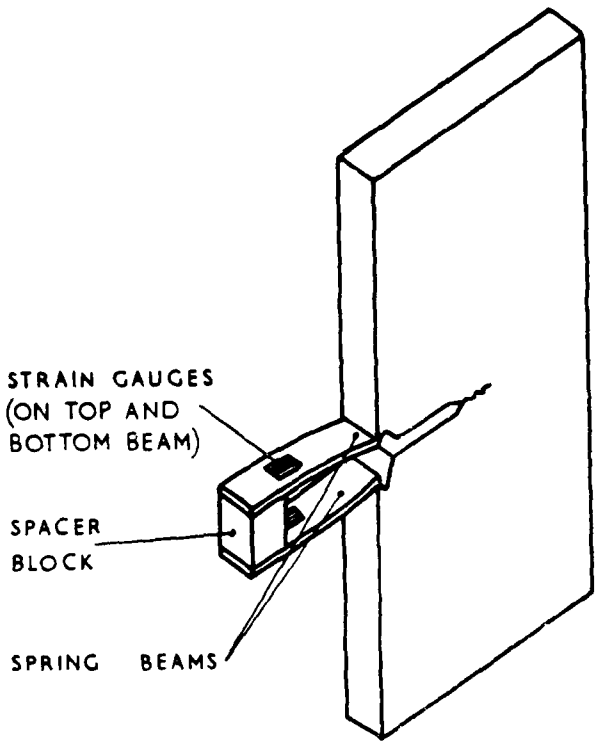

FIG 10 ASTM TYPE STRAIN-GAUGED CLIP GAUGE MOUNTED ON KNIFE EDGES

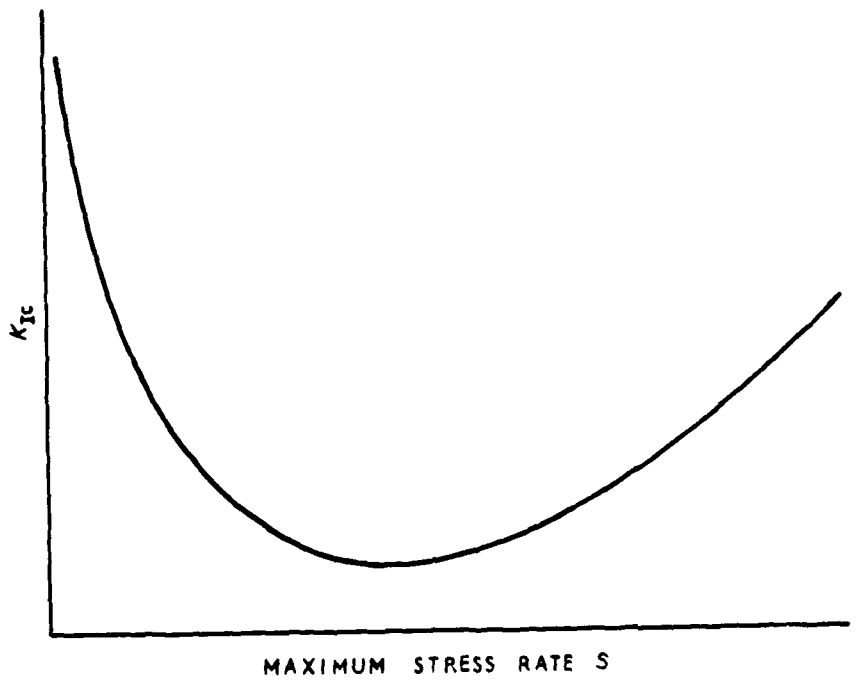

FIG 11 RELATIONSHIP FOR LOW STRENGTH STEELS BETWEEN MAXIMUM STRESS RATE AND K_{Ic}

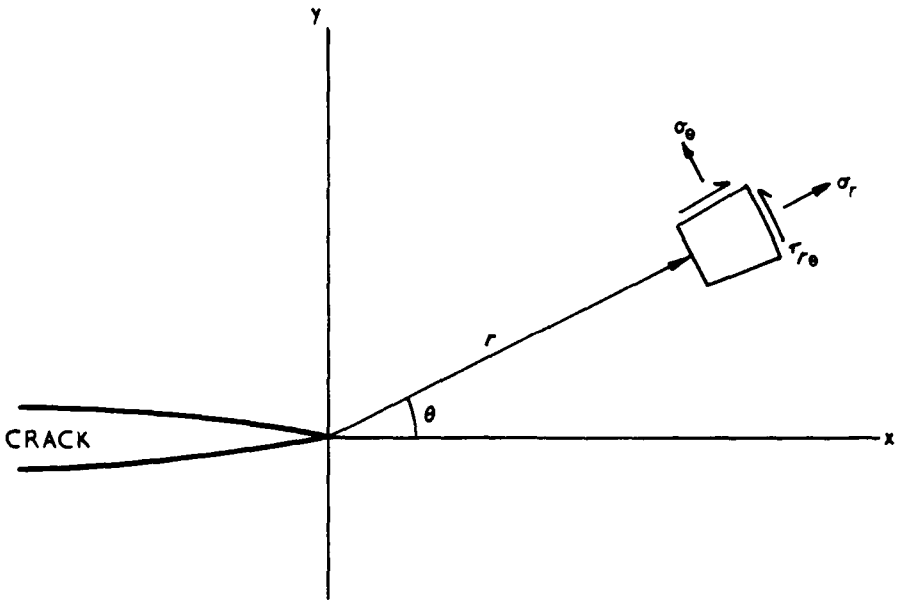

FIG 12 POLAR COORDINATES FOR CRACK TIP STRESS FIELD

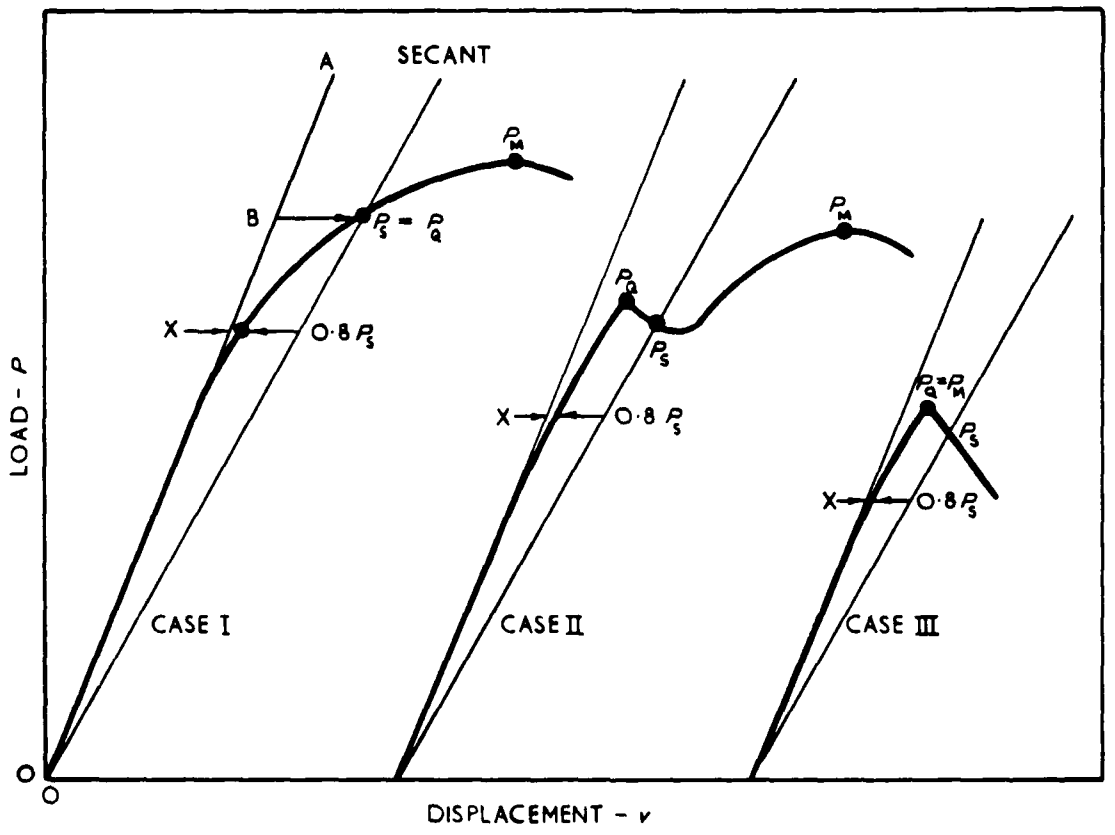

FIG 13 TYPES OF LOAD DISPLACEMENT RECORD ILLUSTRATING OFFSET PROCEDURE FOR DETERMINATION OF K_{Ic}

POOK, L. P.

Linear fracture mechanics – what it is, what it does.

NEL Report No 465. East Kilbride, Glasgow: National Engineering Laboratory. August 1970.
39 pages (9 figures), 30 cm.

This report is intended to assist non-specialists in understanding the numerous specialist papers on linear elastic fracture mechanics. The main concepts are described and the various terms and conventions used are explained. Advanced mathematical techniques are used in fracture mechanics; some of these are described briefly, but results rather than methods are emphasized.

POOK, L. P.

Linear fracture mechanics – what it is, what it does.

NEL Report No 465. East Kilbride, Glasgow: National Engineering Laboratory. August 1970.
39 pages (9 figures), 30 cm.

This report is intended to assist non-specialists in understanding the numerous specialist papers on linear elastic fracture mechanics. The main concepts are described and the various terms and conventions used are explained. Advanced mathematical techniques are used in fracture mechanics; some of these are described briefly, but results rather than methods are emphasized.

POOK, L. P.

Linear fracture mechanics – what it is, what it does.

NEL Report No 465. East Kilbride, Glasgow: National Engineering Laboratory. August 1970.
39 pages (9 figures), 30 cm.

This report is intended to assist non-specialists in understanding the numerous specialist papers on linear elastic fracture mechanics. The main concepts are described and the various terms and conventions used are explained. Advanced mathematical techniques are used in fracture mechanics; some of these are described briefly, but results rather than methods are emphasized.

POOK, L. P.

Linear fracture mechanics – what it is, what it does.

NEL Report No 465. East Kilbride, Glasgow: National Engineering Laboratory. August 1970.
39 pages (9 figures), 30 cm.

This report is intended to assist non-specialists in understanding the numerous specialist papers on linear elastic fracture mechanics. The main concepts are described and the various terms and conventions used are explained. Advanced mathematical techniques are used in fracture mechanics; some of these are described briefly, but results rather than methods are emphasized.

NEL PUBLICATIONS

The following reports are available on request from NEL

FLEMING, I. Graphical aids to part-programming NEL IDI postprocessor, Version 2. *NEL Report* No 450

HENDRY, J. C. Forward extrusion of rod. Calibration tests for the International Cold Forging Group. *NEL Report* No 451

HAYWARD, A. T. J. The role of stabilized gas nuclei in hydrodynamic cavitation inception. *NEL Report* No 452

Direct-contact heat transfer. Report of a meeting at NEL, 15th January, 1969. *NEL Report* No 453

LEIPER, W. and JEATER, J. P. The cavitation characteristics of a venturi section with change of Reynolds and Prandtl number. *NEL Report* No 454

DOWER, R. J. The extrusion moulding process. *NEL Report* No 455

CRUDEN, A. K. and THOMSON, J. F. Extrusion pressures, press loads and tool stresses for the warm extrusion of steel. *NEL Report* No 456

SPEIRS, R. R. M. and WHITAKER, J. An inlet chamber test method for centrifugal fans with ducted outlet. *NEL Report* No 457

SCOTT, D. Metallurgical aspects of materials for tribological applications. *NEL Report* No 458

Index of NEL Publications 1968-1969. *NEL Report* No 459

McKENZIE, J. Lubrication in the cold extrusion of steel. *NEL Report* No 460

WHITAKER, J., BEAN, P. G. and HAY, E. Measurement of losses across multi-cell flow straighteners. *NEL Report* No 461

MARTIN, C. N. B. Computer optimization of Lennard-Jones force constants from experimental data. *NEL Report* No 462

MARTIN, C. N. B. Computer representation of virial coefficient and viscosity for the Stockmayer potential. *NEL Report* No 463

KINGHORN, F. C. The effects of turbulence and transverse velocity gradients on pitot-tube observations. *NEL Report* No 464